Superhard Pseudocubic BC_2N Superlattices

Shiyou Chen and X. G. Gong
Surface Science Laboratory (National Key) and Physics Department, Fudan University, Shanghai 200433, China

Su-Huai Wei
National Renewable Energy Laboratory, Golden, Colorado 80401, USA

(Received 28 June 2006; published 5 January 2007)

It is currently under debate whether diamondlike BC_2N may be harder than cubic BN (*c*-BN). Using the bond counting rule, we have performed an unconstrained search and identified a series of short period (111) superlattices that have much lower total energy than previously proposed structures. By examining the ideal strength of these pseudocubic boron-carbonitrides, we show that they are harder than *c*-BN. Our results are consistent with experimental findings, but in contrast with a recent theoretical study, which claimed that the BC_2N is less hard than *c*-BN.

DOI: 10.1103/PhysRevLett.98.015502 PACS numbers: 62.20.Dc, 61.50.Ah, 61.50.Ks, 62.20.Fe

One of the greatest challenges in materials design is to identify materials that are superhard because these materials have many important mechanical applications [1]. In this pursuit, the alloy of diamond and *c*-BN has recently attracted much interest [2–5]. This is because diamond is the hardest known material, whereas *c*-BN is the second. Therefore, it is hoped that by mixing diamond with *c*-BN, one may create a new pseudodiamond *c*-BC_2N compound that is harder than *c*-BN, but retains the thermal and chemical stability of *c*-BN.

Several successful syntheses of *c*-BC_2N [6–9] have been reported. However, the measured physical properties of the synthesized materials vary significantly. Using shock-wave compression, Komatsu *et al.* [8] obtained *c*-BC_2N with a bulk modulus of 401 GPa, which is larger than that of *c*-BN (~ 369–400 Gpa) [10]. Solozhonko *et al.* [9] synthesized *c*-BC_2N under high pressure and high temperature from graphitelike BC_2N. They found that the sample has both a smaller bulk modulus (282 GPa) and shear modulus (238 ± 8 GPa) [11] than *c*-BN, but it also has a high Vickers hardness (76 GPa), which is only smaller than diamond (~ 100 GPa), but larger than *c*-BN (~ 62 GPa) [3]. The x-ray diffraction measurement [9] showed that the sample exhibits strong 111, 220, and 311 lines of the cubic lattice, and absence of the 200 line, suggesting that the sample has the pseudodiamond structure.

Theoretical investigations of this fascinating material also gave contradictory results, and it is still not clear if BC_2N is harder than *c*-BN. By studying possible synthesis paths for pseudodiamond BC_2N from compression of graphite BC_2N, Tateyama *et al.* [2] proposed an energetically favorable BC_2N structure with a large calculated bulk modulus (438 GPa) and shear modulus (445 GPa) [3], which are only slightly smaller than the values of diamond. Mattesini *et al.* [4,12] proposed several novel orthorhombic and hexagonal BC_2N structures whose shear modulus and bulk modulus are larger than *c*-BN. Based on these calculated elastic moduli at equilibrium, they suggested that these BC_2N structures could be harder than *c*-BN. Gao *et al.* [13], and recently, Antonín Šimůnek *et al.* [14] calculated the hardness of (1×1) (001) BC_2N superlattice [15,16] using empirical formulae based on the bond length, charge density, ionicity, and other properties at equilibrium volume. They find that their results are consistent with experimental observation that BC_2N is harder than *c*-BN [9]. However, their predictions were questioned recently by Zhang *et al.* [17], who demonstrated that the bulk and shear modulus of a material at equilibrium does not necessarily reflect the hardness of the material, because, before the material breaks down, it has severely deformed from its equilibrium position. Therefore, the hardness of a material should be determined by the ideal strength, which is the maximum stress required to break a perfect crystal [17,18]. By searching for the lowest possible total-energy configuration of an eight-atom cubic unit cell, they identified the two most energetically favorable structures (denoted as BC_2N-1 and BC_2N-2, respectively) within the unit cell [19]. They found that, although these two structures have larger shear and bulk modulus than *c*-BN at equilibrium, their ideal tensile and shear strengths are much smaller than that of *c*-BN [17]. Therefore, they argued that *c*-BC_2N is less hard than *c*-BN.

To understand the controversies discussed above, in this Letter, we calculate the total energy, equilibrium lattice parameter, bulk modulus, structure factors, and ideal tensile and shear strength of diamond, *c*-BN, and selected BC_2N structures using first-principles density functional theory. We find that the two *c*-BC_2N structures studied by Zhang *et al.* is at least 1.0 eV per 4 atoms higher than the $(C_2)_n(BN)_n$ (111) superlattice (sl) structures formed by stacking n layers of *c*-BN and n double layers of diamond. This is because the (111) superlattice structures have less "wrong" bonds that do not satisfy the octet rule. The calculated bulk moduli, ideal tensile and shear strengths of the sl-BC_2N are larger than that of *c*-BN, which is consistent with the experimental finding [9] that BC_2N is harder than c-BN, but is in contrast with the claim of Zhang *et al.* that optimal BC_2N is less hard than c-BN [17].

Calculations of the total-energy and stress for this study are carried out using density functional theory as implemented in the ABINIT code [20,21], which is based on pseudopotentials and plane wave basis functions. The norm-conserving Troullier-Martins pseudopotential [22] is used with a cutoff radii of 1.59, 1.49, and 1.50 a.u. for B, C, and N, respectively. We use the local density approximation (LDA) and the exchange-correlation functional of Perdew-Wang parameterized by Goedecker, Teter, and Hutter [23]. For the Brillouin zone integration, we used an $8 \times 8 \times 8$ Monkhorst-Pack k-point grid for an eight-atom cubic unit cell and equivalent k-points for other structures [24]. The cutoff energy for the basis function is 80 Ry.

To calculate the tensile stress, e.g., along the $\langle 111 \rangle$ direction of diamond, we used the standard approach as described in Refs. [18,25]. Specifically, we first apply a small strain in the $\langle 111 \rangle$ direction and conduct the structural optimization for the lattice vectors perpendicular to the $\langle 111 \rangle$ direction and all the internal atomic positions. The minimization is done until the other five components of the stress tensor are all less than 0.1 GPa. The strain is then increased step by step, and at each step, the relaxed structure from the previous step is used as the starting point. The shear stress is computed in a similar way. Here, we first set the desired component of the target shear stress at a certain value and all the other components at zero. After finding the relaxed structure with the given stress, we increase the desired stress step by step until the structure collapses. We take that maximum shear stress as the ideal shear strength.

We first try to identify the crystal structures of BC_2N that have low energies. It is well known for III–V or II–VI semiconductors that when the cation mutates into two cations with one more and one less valence electrons (e.g., $Zn_2Se_2 \rightarrow CuGaSe_2$), the most stable crystal structure is chalcopyrite [Fig. 1(a)], where the anion is surrounded by two cations A and two cations B, thus, satisfying the octet rule [26]. However, in the case of $C_2C_2 \rightarrow BNC_2$, this simple octet rule is not followed, because N is more electronegative than C; thus, B forms stronger bond with N, not with C. Because of this, the most stable structures are the one that maximize the number of the stable B-N and C-C bonds and have no unstable B-B and N-N bonds. After a general search [27] of all pseudo-diamond structures with unit cells less than 4, 8, and 12 atoms, we revealed that the low energy candidates are all the $\langle 111 \rangle$ $((C_2)_n(BN)_n$ superlattices, such as the one shown in Fig. 1(c).

Table I gives the calculated volumes, bulk moduli, and formation energies for diamond, c-BN, $BC_2N_{n\times n}$ ($n = 1$, 2, 3), and the two most stable structures BC_2N-1 and BC_2N-2, proposed in Ref. [17]. Here, $BC_2N_{n\times n}$ denotes the (n, n) (111) superlattice structures. The formation energy is defined as

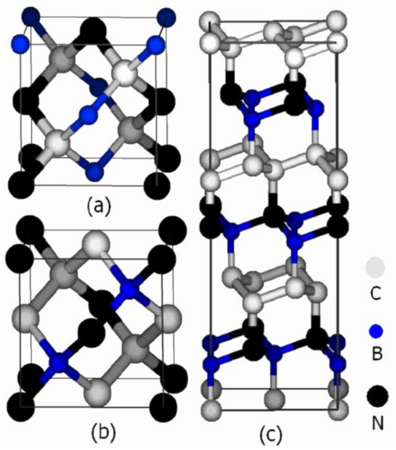

FIG. 1 (color online). Crystal structures of (a) chalcopyrite BC_2N (only half of the body-centered-tetragonal conventional cell is shown), (b) orthorhombic BC_2N-1, and (c) rhombohedral $BC_2N_{1\times1}$ superlattice.

$$\Delta E = E(BC_2N) - E(C_2) - E(BN). \tag{1}$$

We find that (i) all the BC_2N structures have a positive formation energy, suggesting that these structures are metastable with respect to phase separation into the constituents diamond and c-BN at low temperature. (ii) The $BC_2N_{1\times1}$ structure is 1.02 and 1.04 eV per 4-atoms lower in energy than the BC_2N-1 and BC_2N-2 structures, respectively. This indicates that the BC_2N-1 is not the optimal low energy structure of BC_2N, as claimed by Zhang *et al.* [17] The large differences between the formation energy of these structures can be understood by noticing that in the BC_2N-1 or BC_2N-2 structure, the ratio of the less stable B-C and C-N bond and the more stable B-N and C-C bonds is 1:1:1:1, whereas in the $BC_2N_{1\times1}$ structure, the ratio is 1:1:3:3 [Figs. 1(b) and 1(c)]. Because the $BC_2N_{1\times1}$ has fewer B-C and C-N wrong bonds than the BC_2N-1 structure, it is more stable than the BC_2N-1 structure. (iii) The

TABLE I. Calculated volume V, bulk modulus B, and formation energy ΔE for diamond, c-BN, and some of the BC_2N structures studied in this Letter.

Structure	V ($Å^3/4-$ atoms)	B (GPa)	ΔE (eV/4-atoms)
Diamond	22.22	454	⋯
c-BN	23.19	392	⋯
$BC_2N_{1\times1}$	22.92	419.5	0.76
$BC_2N_{2\times2}$	22.84	419.5	0.52
$BC_2N_{3\times3}$	22.80	421.9	0.39
BC_2N-1	23.06	397.6	1.78
BC_2N-2	23.06	400.2	1.80

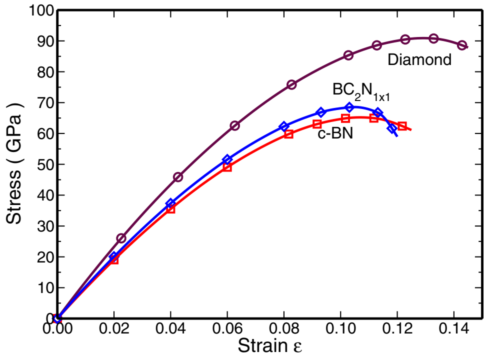

FIG. 2 (color online). Calculated tensile stress as a function of the strain ϵ for diamond, *c*-BN, and $BC_2N_{1\times1}$.

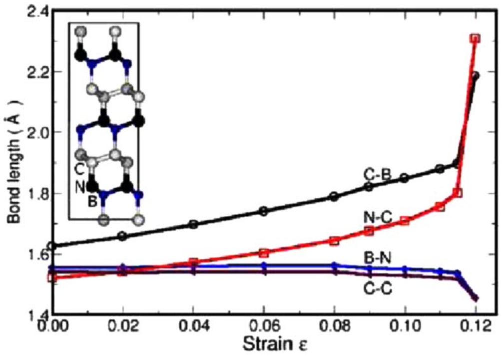

FIG. 3 (color online). Calculated bond lengths as a function of the tensile strain ϵ of $BC_2N_{1\times1}$.

formation energy decreases (i.e., becomes more stable) as n increases, because the ratio is 1:1:4n-1:4n-1 (i.e., as n increases, there are more C-C and B-N bonds and fewer B-C and C-N bonds). This is consistent with the fact that the phase separation into diamond and *c*-BN is the most stable one. In the following discussion, we will focus only on the ultrathin (111) superlattices.

Experimentally, it is found that the BC_2N sample is diamondlike; i.e., it has a very weak 200 x-ray diffraction line [9]. Because the x-ray diffraction intensity is proportional to the structure factor squared, $|\rho(\mathbf{G})|^2$, we have calculated the structure factors for diamond, *c*-BN and $BC_2N_{1\times1}$, and compared them with those of BC_2N-1 or BC_2N-2 structures using the all-electron linearized augmented plane wave method [28]. We find that for all the BC_2N structures, the 200 structure factor is weak because the atomic number of B and N is close to C. The calculated 200 intensity for (1×1) superlattice is about 3 times smaller than the BC_2N-1 and BC_2N-2 structures. In this sense, it is more "cubic" than the two previously proposed structures, and therefore is more consistent with experimental observations [9].

All the sl-BC_2N structures listed in Table I have a larger bulk modulus than *c*-BN, indicating that the superlattice is more difficult to compress than *c*-BN near their respective equilibrium volumes. To see if these sl-BC_2N are also harder than *c*-BN, we follow the arguments of Zhang *et al.* to calculate their ideal strengths. In Fig. 2, we show the tensile stress as a function of strain for diamond and *c*-BN along the $\langle 111\rangle$ direction, which is known to be the weakest direction. The calculated ideal tensile strength is 90.8 GPa at a strain $\epsilon = 0.13$ for diamond and 65.2 GPa at a strain $\epsilon = 0.11$ for *c*-BN, which is consistent with previous calculations [17,18,29,30]. As a comparison, $BC_2N_{1\times1}$ along the $\langle 111\rangle$ direction has an ideal strength of 68.4 GPa at strain $\epsilon = 0.10$. To verify that the superlattice $\langle 111\rangle$ direction is indeed the weakest direction of $BC_2N_{1\times1}$, we have also calculated the tensile stresses along three other directions, $\langle\bar{1}10\rangle$, $\langle\bar{1}\,\bar{1}\,2\rangle$, and $\langle\bar{1}11\rangle$. The first two are orthogonal to the $\langle 111\rangle$ direction. We find that, like in diamond and *c*-BN, the stress along the superlattice $\langle 111\rangle$ direction indeed has the smallest maximum.

Our results show that the ideal tensile strength of the energetically favorable $BC_2N_{1\times1}$ is larger than *c*-BN, thus indicating that it could be harder than *c*-BN [17]. To further confirm this, we have also calculated the ideal shear strengths [3] for *c*-BN and $BC_2N_{1\times1}$, where the shear is applied along the $\langle\bar{1}\,\bar{1}\,2\rangle$ direction, perpendicular to the $\langle 111\rangle$ direction. We find that the ideal shear strength of $BC_2N_{1\times1}$ is 65.6 GPa, larger than the value of 62.0 GPa for *c*-BN. This confirms that $BC_2N_{1\times1}$ is indeed harder than *c*-BN, as well as the two BC_2N structures proposed by

TABLE II. Calculated ideal tensile strength and the corresponding strain at which the maximum stress (in GPa) occurs. The results are compared with previous calculations [17].

Structure	Direction	Strain	Stress	Stress [17]
Diamond	$\langle 111\rangle$	0.130	90.8	92.8
c-BN	$\langle 111\rangle$	0.108	65.2	65.0
$BC_2N_{1\times1}$	$\langle 111\rangle$	0.103	68.4	
$BC_2N_{2\times2}$	$\langle 111\rangle$	0.105	73.4	
$BC_2N_{3\times3}$	$\langle 111\rangle$	0.100	72.0	
BC_2N-1	$\langle\bar{1}11\rangle$	0.053	33.0	35.0
BC_2N-2	$\langle 111\rangle$	0.078	53.4	55.7

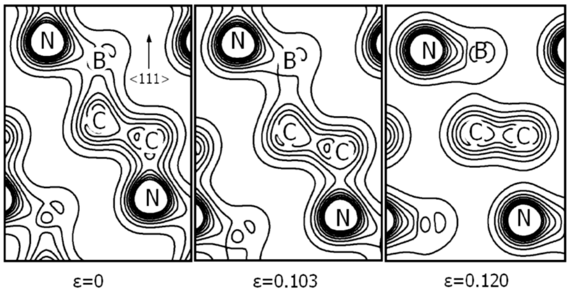

FIG. 4. Calculated charge density in the $\langle\bar{1}10\rangle$ plane of $BC_2N_{1\times1}$ at tensile strain $\epsilon = 0$, 0.103, 0.120 parallel to the $\langle 111\rangle$ direction.

Zhang *et al.*, whose calculated ideal tensile strengths are also shown in Table II.

Figure 3 plots the calculated bond length of $BC_2N_{1\times1}$ as a function of the $\langle 111 \rangle$ tensile strain. We see that the in-plane C-C and B-N bond lengths are not sensitive to the strain. The B-C and C-N bonds parallel to the $\langle 111 \rangle$ direction elongate with the strain. The slope increases drastically just before the bonds along the $\langle 111 \rangle$ direction start to break at $\epsilon = 0.12$. After the bond breaks, the system converts into a planar structure with alternating graphite and hexagonal BN layers. Figure 4 shows the valence charge density of $BC_2N_{1\times1}$ at equilibrium, at maximum stress, and just after the bonds break. Following the evolution of the charge density, we find that the weak C-N bond starts to break first, followed by the B-C bond. Further investigation showed that the C-N bond is weakened at high strain by hybridizing with the high lying antibonding state, which is localized at the donorlike C-N bond.

For thicker $\langle 111 \rangle$ superlattices, the ideal tensile strength along the $\langle 111 \rangle$ direction increases to 73.4 GPa for $BC_2N_{2\times2}$, but decreases to 72.0 GPa for $BC_2N_{3\times3}$ (Table II). Furthermore, we find that the parallel C-C bond at the C-N interface, which does not exist in the (1×1) superlattice, is weakened significantly at large strain and starts to break together with the C-N bond. These variations of the ideal strength and the breakdown of the C-C bond at the interface can be understood by noticing that the breaking of the bond is caused by mixing of the antibonding charge character into the bond to restore the nonbonding atomic character of the orbital. The mixing of the antibonding charge character increases when the energy separation between the occupied bonding state and unoccupied antibonding states decreases. We find that this antibonding state has its charge localized near the donorlike C-N/C-C interface. Its energy increases from $n = 1$ to $n = 2$ due to the reduced $\Gamma - L$ coupling, but decreases when n further increases due to reduced quantum confinement [31]. This explains the trend of the ideal strength as a function of superlattice period n and why the bonds at the C-C/C-N bond start to break first.

In summary, using the bond counting rule, we have identified a series of short period $(C_2)_n(BN)_n$ (111) superlattices that have low energies and could be harder than *c*-BN. We suggest that these metastable ultrathin (111) superlattices could be grown using low-temperature vapor phase epitaxial methods. The need for experimental study to test our predictions is indicated.

The work at Fudan University is partially supported by the National Science Foundation of China, the Special Funds for Major State Basic Research, and the Shanghai Project. The computation is performed in the Supercomputer Center of Shanghai, the Supercomputer Center of Fudan University, and CCS. The work at NREL is funded by the U.S. Department of Energy, under Contract No. DE-AC36-99GO10337.

[1] M. L. Cohen, Science **261**, 307 (1993).
[2] Y. Tateyama, T. Ogitsu, K. Kusakabe, S. Tsuneyuki, and S. Itoh, Phys. Rev. B **55**, R10161 (1997).
[3] D. M. Teter, Mater. Res. Bull. **23**, 22 (1998).
[4] M. Mattesini and S. F. Matar, International Journal of Inorganic Materials **3**, 943 (2001).
[5] R. B. Kaner, J. J. Gilman, and S. H. Tolbert, Science **308**, 1268 (2005).
[6] S. Nakano, M. Akaishi, T. Sasaki, and S. Yamaoka, Chem. Mater. **6**, 2246 (1994).
[7] E. Knittle, R. B. Kaner, R. Jeanloz, and M. L. Cohen, Phys. Rev. B **51**, 12 149 (1995).
[8] T. Komatsu, M. Nomura, Y. Kakudate, and S. Fujiwara, J. Mater. Chem. **6**, 1799 (1996).
[9] V. L. Solozhenko, D. Andraut, G. Fiquet, M. Mezouar, and D. C. Rubie, Appl. Phys. Lett. **78**, 1385 (2001).
[10] A. Janotti, S.-H. Wei, and D. J. Singh, Phys. Rev. B **64**, 174107 (2001).
[11] S. N. Tkachev, V. L. Solozhenko, P. V. Zinin, M. H. Manghnani, and L. C. Ming, Phys. Rev. B **68**, 052104 (2003).
[12] M. Mattensini and S. F. Matar, Comput. Mater. Sci. **20**, 107 (2001).
[13] F. Gao, Phys. Rev. Lett. **91**, 015502 (2003).
[14] A. Šimunek and J. Vackář, Phys. Rev. Lett. **96**, 085501 (2006).
[15] W. R. L. Lambrecht and B. Segall, Phys. Rev. B **40**, 9909 (1989).
[16] R. Q. Zhang, K. S. Chan, H. F. Cheung, and S. T. Lee, Appl. Phys. Lett. **75**, 2259 (1999).
[17] Y. Zhang, H. Sun, and C. Chen, Phys. Rev. Lett. **93**, 195504 (2004).
[18] D. Roundy and M. L. Cohen, Phys. Rev. B **64**, 212103 (2001).
[19] H. Sun, S. H. Jhi, D. Roundy, M. L. Cohen, and S. G. Louie, Phys. Rev. B **64**, 094108 (2001).
[20] X. Gonze *et al.*, Comput. Mater. Sci. **25**, 478 (2002).
[21] X. Gonze *et al.*, Z. Kristallogr. **220**, 558 (2005).
[22] N. Troullier and J. L. Martins, Phys. Rev. B **43**, 1993 (1991).
[23] S. Goedecker, M. Teter, and J. Hutter, Phys. Rev. B **54**, 1703 (1996).
[24] H. J. Monkhorst and J. D. Pack, Phys. Rev. B **13**, 5188 (1976).
[25] D. Roundy, C. R. Krenn, M. L. Cohen, and J. W. Morris, Philos. Mag. A **81**, 1725 (2001).
[26] S.-H. Wei, L. G. Ferreira, and A. Zunger, Phys. Rev. B **45**, 2533 (1992).
[27] L. G. Ferreira, S.-H. Wei, and A. Zunger, International Journal of Supercomputer Applications and High Performance Computing **5**, 34 (1991).
[28] S.-H. Wei and H. Krakauer, Phys. Rev. Lett. **55**, 1200 (1985).
[29] R. H. Telling, C. J. Pickard, M. C. Payne, and J. E. Field, Phys. Rev. Lett. **84**, 5160 (2000).
[30] H. Chacham and L. Kleinman, Phys. Rev. Lett. **85**, 4904 (2000).
[31] T. Mattila, S.-H. Wei, and A. Zunger, Phys. Rev. Lett. **83**, 2010 (1999).